THE JOURNAL OF PHYSICAL CHEMISTRY C

Article

pubs.acs.org/JPCC

Solvent Effects on the Adsorption Geometry and Electronic Structure of Dye-Sensitized TiO_2: A First-Principles Investigation

Edoardo Mosconi,[†,‡] Annabella Selloni,*[,§] and Filippo De Angelis*[,‡]

[†]Dipartimento di Chimica, Università degli Studi di Perugia, via Elce di Sotto 8, I-06123, Perugia, Italy

[‡]Istituto CNR di Scienze e Tecnologie Molecolari (ISTM), c/o Dipartimento di Chimica, Università di Perugia, Via elce di Sotto 8, I-06123, Perugia, Italy

[§]Department of Chemistry, Princeton University, New Jersey, 08544, United States

Supporting Information

ABSTRACT: The performance of dye-sensitized solar cells (DSSCs) depends significantly on the adsorption geometry of the dye on the semiconductor surface. In turn, the stability and geometry of the adsorbed molecules is influenced by the chemical environment at the electrolyte/dye/TiO_2 interface. To gain insight into the effect of the solvent on the adsorption geometries and electronic properties of dye-sensitized TiO_2 interfaces, we carried out first-principles calculations on organic dyes and solvent (water or acetonitrile) molecules coadsorbed on the (101) surface of anatase TiO_2. Solvent molecules introduce important modifications on the dye adsorption geometry with respect to the geometry calculated in vacuo. In particular, the bonding distance of the dye from the Ti anchoring atoms increases, the adsorption energy decreases, and the two C−O bonds in the carboxylic moieties become more symmetric than in vacuo. Moreover, the adsorbed solvent induces the deprotonation of the dye due to the changing the acid/base properties of the system. Analysis of the electronic structure for the dye-sensitized TiO_2 structures in the presence of coadsorbed solvent molecules shows an upward shift in the TiO_2 conduction band of 0.2 to 0.5 eV (0.5 to 0.8 eV) in water (acetonitrile). A similar shift is calculated for a solvent monolayer on unsensitized TiO_2. The overall picture extracted from our calculations is consistent with an upshift of the conduction band in acetonitrile (2.04 eV vs SCE) relative to water (0.82 eV vs SCE, pH 7), as reported in previous studies on TiO_2 flatband potential (Redmond, G.; Fitzmaurice, D. *J. Phys. Chem.* **1993**, *97*, 1426−1430) and suggests a relevant role of the solvent in determining the dye−semiconductor interaction and electronic coupling.

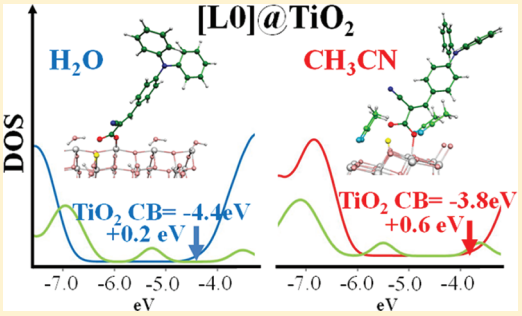

1. INTRODUCTION

Dye-sensitized solar cells (DSSCs) are promising devices for high-efficiency, low-cost solar energy conversion.[1−5] In DSSCs, TiO_2 nanoparticles are sensitized with light-harvesting dyes, which are typically surrounded by a liquid-phase electrolyte containing the I^-/I_3^- redox pair[6−8] and acetonitrile (CH_3CN) as solvent.[9,10] Extensive research on DSSCs has shown that the adsorption mode of the dye on the semiconductor plays a very important role in the device performance.[11,12] DSSCs are generally fabricated under normal atmospheric conditions. In this environment, humidity is always present. Thus DSSCs always contain a certain amount of water in their constituting materials. Moreover, the permeation of water at the sealing of the DSSCs increases the water content in the electrolyte over time.[13]

In previous experimental studies,[14−21] water was deliberately added to the DSSCs, either by direct addition to the solvent used for the DSSC assembly or by pretreatment of TiO_2 with water. Reports on the effects of this addition have been somewhat controversial. An increase in the device efficiency has been sometimes observed, which was explained by a decrease in the recombination due to blocking of the TiO_2 surface by adsorbed water or by a reduced amount of I_3^- on the TiO_2 due to the higher solubility of the electrolyte.[14−16] However, a decrease in the short circuit current density has been also reported, which was attributed either to desorption of the dye from the TiO_2 surface into the solution or to a decrease in the dye−TiO_2 interaction.[16] In yet another study,[18] TiO_2 electrodes sensitized with N3, N719, and Z907 were exposed to water, and the DSSCs performances were measured. It was found that the hydrophilic chain of the Z907 dye effectively protects the TiO_2 surface against water adsorption, whereas the presence of water reduces the amount of N3 and N719 molecules on the TiO_2 surface. Moreover, a change in the dye orientation at the surface was observed, with a rearrangement of thiocyanate ligands toward the TiO_2 surface. In general, a decrease in the DSSCs performance is found when the amount of water exceeds 10%.[21] For this reason, the cell is usually sealed to prevent water permeation into the electrolyte. Desorption of the dye induced by the presence of water was observed also in a

Received: September 29, 2011
Revised: February 8, 2012
Published: February 8, 2012

   dx.doi.org/10.1021/jp209420h | *J. Phys. Chem. C* 2012, 116, 5932−5940

recent Car–Parrinello molecular dynamics simulation.[22] Vice versa, the solvent that has provided the best results in terms of DSSCs efficiency is acetonitrile.[9,23]

The electrochemical properties of TiO_2 are also strongly influenced by the solvent. In water, a Nernstian dependence of the semiconductor flat-band potential on pH is observed; the flat-band potential shifts to more negative potentials (vs SCE) by 0.06 V for every pH unit increase, according to the equation: V_{fb}(V, SCE) = −0.40 − (0.06pH). In the presence of acetonitrile, TiO_2 flat-band potential measurements by Fitzmaurice and coworkers[24−27] have shown that the TiO_2 conduction band undergoes an upward shift in comparison with water.[24] In particular, a flat-band potential of 2.04 V versus SCE was reported for a carefully dehydrated acetonitrile solution,[24] whereas in water at pH 7 a TiO_2 flat-band potential of 0.82 V vs SCE is expected. This large and somewhat surprising difference suggests an important solvent effect on the position of the TiO_2 manifold of unoccupied states.

Numerous theoretical investigations have examined the adsorption mode of small organic molecules (i.e., formic acid[28−32] and benzoic acid,[33] isonicotinic acid,[34] and bipyridine ligand[35]), small phosphonate group,[36] metal-free organic dyes,[11,37−39] and ruthenium-complex[12,40−42] dyes on TiO_2. The overall picture extracted from these works indicates an important role of the dye adsorption energy and geometry on the electrochemical properties and the DSSCs efficiency. Previous theoretical studies have also focused on the characterization of the solvent-TiO_2 interactions (water[43−46] and acetonitrile[47−50,44]) in both free and dye-sensitized TiO_2. However, a systematic study of the solvent−dye−TiO_2 heterointerface, comparing water and acetonitrile solvents, and of the associated structural and electronic changes is still missing.

In this work, we use first-principles density functional theory (DFT) calculations to investigate the effect of the explicit solvent on the adsorption geometries and electronic properties of prototypical dyes adsorbed onto TiO_2 anatase surfaces. Focusing on three representative prototype organic dye molecules, benzoic acid ([BA]), 2-cyano-3-phenyl-acrylic acid ([CA]), and the 4-(diphenylamino)phenylcyanoacrylic acid dye ([L0]) (see Scheme 1), we examine the effect of both water and acetonitrile solvents on their atomic and electronic structures. [BA] is the typical anchoring group of bipyridine ligands in the widely employed Ru(II) dyes. Investigation of [BA] adsorption on TiO_2 allows us to establish the setup and to check our theoretical approach by comparing our results to previously published calculations.[33] As for the other dyes considered in this study, [CA] shows the typical cyanoacrylic anchoring/acceptor group of push−pull organic dyes, whereas [L0] represents a prototype push−pull organic dye used in DSSC, characterized by a triphenylamine donor moiety and by a cyanoacrylic acid acceptor group.[51,52]

Scheme 1. Chemical Structures of the Investigated Molecules: Benzoic Acid [BA], 2-Cyano-3-phenyl-acrylic acid ([CA]), and 4-(Diphenylamino)phenylcyanoacrylic Acid [L0]

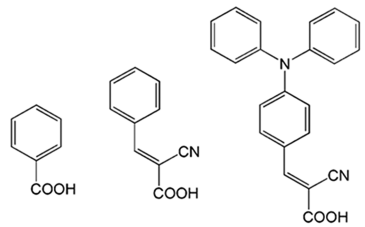

2. METHODS

Periodic DFT calculations have been carried out within the generalized gradient approximation (GGA) using the PBE exchange-correlation functional.[53] The Car–Parrinello (CP) code as implemented in Quantum-Espresso package was used.[54] Electron–ion interactions were described by ultrasoft pseudopotentials with electrons from O, N, and C 2s, 2p; H 1s; and Ti 3s, 3p, 3d, 4s shells explicitly included in the calculations. Plane-wave basis set cutoffs for the smooth part of the wave functions and the augmented density were 25 and 200 Ry, respectively.

The TiO_2 anatase (101) surface was modeled as a periodic three-layers slab of oxide containing 48 TiO_2 units with eight reactive Ti sites on both sides. The molecules were adsorbed on one side only of the slab, and the vacuum between the top of the molecules and the adjacent slab was ∼7 Å. As shown in ref 33a, a three-layer TiO_2 slab represents a good model for the investigation of benzoic acid adsorption; in particular, computed binding energies are almost independent of the number of layers in the anatase slabs.[33a] A damped dynamics was used for geometry optimizations with force threshold of 1.0×10^{-4} atomic units. The adsorbed molecules and all atoms of the slab were allowed to relax. Using the optimized geometries, electronic structure calculations were performed to obtain the projected densities of states (PDOS). In the absence of coadsorbed solvent molecules, the dye adsorption energies were simply calculated as: $E_{ads} = E_{[slab\text{-}dye]} - E_{[dye]} - E_{[slab]}$, where $E_{[slab\text{-}dye]}$, $E_{[slab]}$, and $E_{[dye]}$ are the energies of the adsorbate-covered slab, the relaxed bare slab, and the gas-phase molecule, respectively. In the presence of the solvent, the dye adsorption energy is calculated as: $E_{ads} = E_{[slab\text{-}solv\text{-}dye]} - E_{[dye]} - E_{[slab\text{-}solv]}$, where $E_{[slab\text{-}solv\text{-}dye]}$ is the energy of the slab with the adsorbed dye and adsorbed solvent and $E_{[slab\text{-}solv]}$ is the energy of the slab with the same number of adsorbed solvent molecules as in $E_{[slab\text{-}solv\text{-}dye]}$.

We also performed selected test calculations of [BA] adsorbed on a $(TiO_2)_{38}$ cluster using the ADF program,[55] with the PBE functional and a TZP (DZP) basis set for Ti (O,C, H). The $(TiO_2)_{38}$ nanoparticle[56−58] was modeled by appropriately "cutting" an anatase slab exposing the majority (101) surface.[59] If not otherwise stated, we shall refer to Car–Parrinello optimized geometries.

3. ADSORPTION STRUCTURES

We first consider the possible bidentate and monodentate adsorption modes of [BA], [CA] and [L0] in vacuo; see Scheme 2. We have identified four different adsorption modes: bidentate, **1**, and monodentate, **2**, **3**, and **4**, either molecular or dissociative. Starting from the geometries optimized in vacuo, we added the solvent molecules, water or acetonitrile, so as to saturate all of the reactive five-fold coordinated Ti sites on the TiO_2 surface.

3.1. Bidentate Adsorption Mode. In the bidentate structure **1**, Figure 1(here and in the following Figures for adsorbed [LO] are presented), both carboxylic oxygen atoms (O1 and O2) are bound to two five-fold coordinated Ti atoms,

dx.doi.org/10.1021/jp209420h | J. Phys. Chem. C 2012, 116, 5932−5940

Scheme 2. Schematic Representation of the Possible Adsorption Modes of [L0] on TiO_2[a]

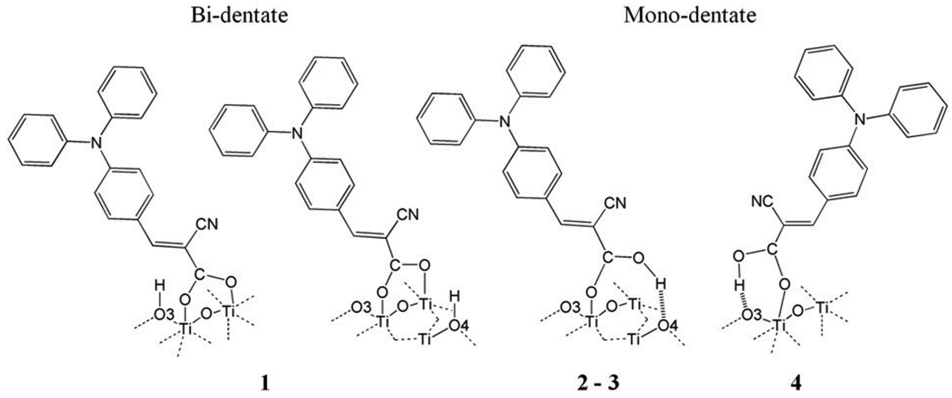

[a]We use the same labels also for [BA] and [CA] adsorbates.

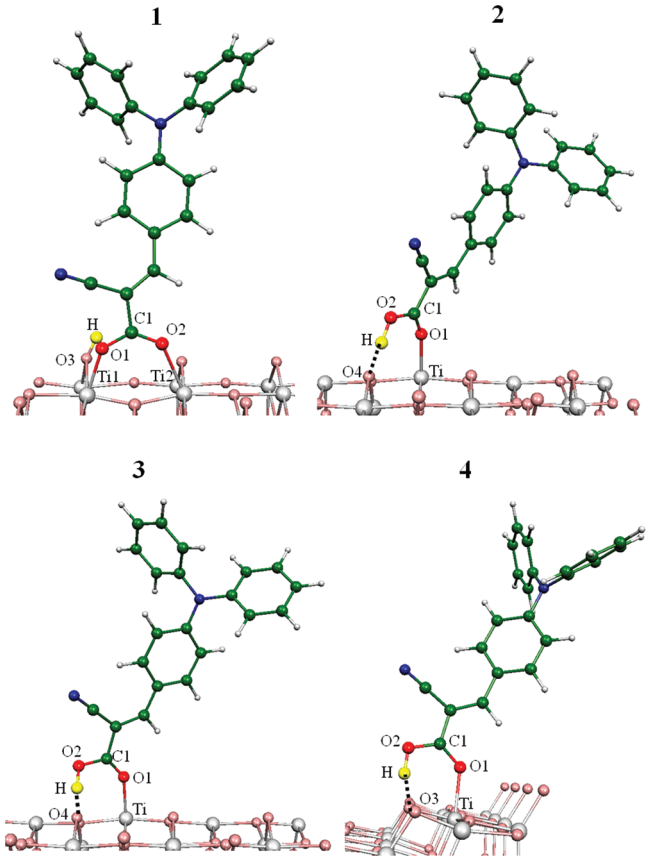

Figure 1. Optimized adsorption structures of [L0]: bidentate **1**; molecular monodentate **2**, **3**, and **4**.

whereas the acid hydrogen atom (H) is bonded to the bridging O3 oxygen on the TiO_2 surface. As shown in Table 1, the Ti1−O1 and Ti2−O2 bond distances in vacuo are not symmetric, showing differences of 0.08, 018, and 0.24 Å for [BA], [CA], and [L0], respectively. The C1−O1 and C1−O2 distances are more symmetric, showing differences of ca. 0.02, 0.03, and 0.04 Å for [BA], [CA], and [L0], respectively.

By adding a layer of water molecules, the Ti1−O1 and Ti2−O2 distances increase by 0.06 and 0.04 Å for [BA], by 0.05 and 0.08 Å for [CA], and by 0.05 and 0.07 Å for [L0], whereas the slight asymmetry of the O1−C1 and O2−C1 bonds is further decreased. However, the main difference between the geometry in vacuo and the geometry in the presence of coadsorbed water is that the more stable position of the proton changes from O3 to the O4 oxygen atom; see Scheme 2.

In the presence of a layer of acetonitrile molecules, we observe a further elongation of the Ti1−O1 and Ti2−O2 distances with respect to the geometry in water. The changes are 0.09 and 0.12 Å for [BA], 0.15 and 0.21 Å for [CA], and 0.12 and 0.24 Å for [L0].

3.2. Monodentate Adsorption Modes. The molecular monodentate structure **2** (Figure 1) is characterized in vacuo by a Ti−O1 bond and hydrogen-bond interaction between H and the O4 oxygen atom belonging to the TiO_2 slab. From Table 1, we can see that the O1−C1 and O2−C1 bond lengths are asymmetrical: the O2−C1 distance is ∼1.26 Å, indicating a carbonyl bond, whereas O2−C1 is about 1.32 to 1.31 Å, indicating a hydroxylic bond. The dihedral < O1−C1−O2−H angle indicates that the carboxylic moiety is nearly planar. The structural parameters in the presence of coadsorbed water, see Figure 2 and Table 1, are similar to those in vacuo except for an elongation of the Ti−O1 bond length of 0.06, 0.07, and 0.07 Å for [BA], [CA], and [L0], respectively. There is also a slight elongation of the O2−H distance ranging from 0.02 Å for [BA] to 0.05 Å for [L0], indicating a modification of the system acid/base properties. By adding a layer of acetonitrile, structure **2** changes from molecular monodentate to dissociative monodentate; see Figure 3. The deprotonated carboxylic moiety is characterized by an O2−H distance in the range of 1.43 Å for [BA] to 1.37 Å for [L0], whereas the distance between the acid hydrogen (H) and the O4 oxygen of TiO_2 slab is about 1.05 to 1.07 Å. The O1−C1 and O2−C1 distance are completely symmetric in the presence of acetonitrile, about 1.27 to 1.28 Å for all the investigated species.

The monodentate structure **3** in vacuo (Figure 1) is similar to the structure **2** except for the dihedral < O1−C1−O2−H angle. In this case, the proton is out of the plane described by O1, C1, and O2 atoms by a value between 20 and 45° going from [BA] to [L0]; see Table 1. By adding one layer of water molecules, we obtain a dissociated monodentate structure with the proton adsorbed on the O4 oxygen of TiO_2 surface. As shown in Figure 2, the deprotonation is promoted by the stabilizing hydrogen-bond interaction between the hydrogen belonging to one adsorbed vicinal water molecule (Hw) and the O2 oxygen belonging to the organic dye. The O1−C1 and O2−C1 distances are substantially symmetric, showing a value around 1.28 Å for all investigated systems; see Table 1. The deprotonation of the molecular carboxylic group also occurs in

dx.doi.org/10.1021/jp209420h | J. Phys. Chem. C 2012, 116, 5932−5940

Table 1. Main Optimized Geometrical Parameters of the Investigated Systems on TiO_2

	[BA]			[CA]			[L0]		
distance (Å), angle (degree)	vac.	wat.	ac.	vac.	wat.	ac.	vac.	wat.	ac.
Adsorption Mode 1									
Ti1−O1	2.040	2.102	2.133	2.021	2.074	2.168	1.990	2.040	2.114
Ti2−O2	2.121	2.159	2.242	2.207	2.292	2.416	2.230	2.298	2.470
O1−C1	1.299	1.287	1.290	1.298	1.288	1.280	1.307	1.295	1.296
O2−C1	1.278	1.286	1.272	1.271	1.273	1.269	1.271	1.274	1.261
C1−C2	1.491	1.500	1.514	1.500	1.512	1.531	1.491	1.501	1.523
O3−H	0.97	0.977	0.978	0.97	0.977	0.950	0.97	0.977	0.978
<Ti1−O1−C1−C2	157	152	167	155	147	155	153	146	164
Adsorption Mode 2									
Ti−O1	2.142	2.198	2.220	2.192	2.265	2.377	2.105	2.174	2.303
O1−C1	1.258	1.253	1.278	1.255	1.250	1.270	1.264	1.257	1.271
O2−C1	1.317	1.319	1.273	1.313	1.313	1.272	1.311	1.309	1.275
C1−C2	1.485	1.491	1.516	1.492	1.501	1.534	1.472	1.482	1.541
O2−H	1.040	1.061	1.425	1.045	1.082	1.439	1.052	1.098	1.365
O4−H	1.517	1.456	1.059	1.482	1.390	1.052	1.433	1.330	1.072
<O1−C1−O2−H	9	7	2	9	8	12	17	17	14
Adsorption Mode 3									
Ti−O1	2.154	2.116	2.296	2.263	2.223	2.404	2.155	2.077	2.276
O1−C1	1.259	1.281	1.280	1.255	1.270	1.268	1.264	1.280	1.272
O2−C1	1.318	1.284	1.273	1.319	1.287	1.271	1.323	1.282	1.259
C1−C2	1.485	1.499	1.518	1.493	1.508	1.529	1.471	1.492	1.509
O2−H	1.043	1.571	1.398	1.047	1.533	1.409	1.051	1.493	1.384
O4−H	1.486	1.015	1.057	1.457	1.019	1.049	1.441	1.031	1.049
O2−Hw		1.607			1.599			1.856	
<O1−C1−O2−H	20	62	37	32	62	27	45	49	38
Adsorption Mode 4									
Ti−O1	2.132	2.189	2.120	2.182	2.194	2.206	2.134	2.190	2.188
O1−C1	1.267	1.265	1.282	1.265	1.278	1.272	1.273	1.271	1.274
O2−C1	1.318	1.315	1.277	1.316	1.290	1.278	1.318	1.311	1.281
C1−C2	1.477	1.485	1.508	1.483	1.502	1.520	1.467	1.478	1.508
O2−H	1.052	1.104	1.547	1.059	1.282	1.507	1.056	1.129	1.461
O3−H	1.454	1.353	1.024	1.427	1.139	1.029	1.414	1.287	1.039
<O1−C1−O2−H	0	1	0	0	0	0	2	2	2

the presence of acetonitrile, with O2−H (O4−H) distances of 1.40 (1.06), 1.41 (1.05), and 1.38 (1.05) Å for [BA], [CA], and [L0], respectively. In this case, the deprotonation is not induced by the hydrogen-bond stabilization but by the increase in the basic character of the solvated TiO_2 surface due to the acetonitrile adsorption. In particular, the donor effect of the acetonitrile adsorption increases the basicity of the TiO_2 oxygen atoms and makes possible the proton transfer from the dye to the oxide surface. Also, in this case, we find an increase in the Ti1−O1 distance with respect to the values in vacuo and symmetric O1−C1 and O2−C1 distances.

The monodentate structure **4** (see Figure 1) is characterized by Ti1−O1 distances of 2.13, 2.18, and 2.13 Å for [BA], [CA], and [L0], respectively, and a hydrogen bond between the proton and the O3 surface oxygen atom, which is directly bonded to the Ti atom. Whereas very similar structures are calculated for the cluster models of **1** and **2** using the CP and ADF programs (see Supporting Information), for the cluster model of **4** the ADF-optimized structure shows the proton to be transferred to the surface, whereas in the CP-optimized structure the proton is retained in the [BA] carboxylic group as in the periodic boundary conditions optimized structure; see the Supporting Information. In the presence of coadsorbed water molecules (Figure 2), an elongation of the Ti−O1 and O2−H distances is observed. In particular, whereas [BA] and [L0] show only an elongation of the O2−H bond (by 0.05 and 0.07 Å, respectively), for [CA], we find a partial deprotonation of the carboxylic moiety with an O2−H distance of 1.28 and an O3−H distance of 1.14 Å. Also, in this case, the presence of acetonitrile induces the complete deprotonation of the carboxylic group of the molecules, with O2−H (O4−H) distances of 1.55 (1.02), 1.51 (1.03), and 1.46 (1.04) Å for [BA], [CA], and [L0], respectively. We also find an increase in the Ti1−O1 distances with respect to their values in vacuo as well as fully symmetric O1−C1 and O2−C1 distances with a length of 1.27 Å for all investigated species.

4. ADSORPTION ENERGIES

The computed adsorption energies for all investigated structures of [BA], [CA], and [L0] are reported in Table 2. The most stable adsorption structure in vacuo is the molecular monodentate structure **4**, which gives adsorption energies of −21.1, −20.6, and −23.4 kcal/mol for [BA], [CA], and [L0] respectively. The [L0] dye shows the highest adsorption energy in vacuo, most likely because of the presence of the nitrogen-donor moiety, which increases the charge donation from the dye to the TiO_2 surface through the Ti−O bonds. Our results compare favorably with those of previous theoretical studies. In particular, our computed adsorption energy for [BA] in vacuo is in good agreement with the result of ref 33, and the adsorption

dx.doi.org/10.1021/jp209420h | J. Phys. Chem. C 2012, 116, 5932−5940

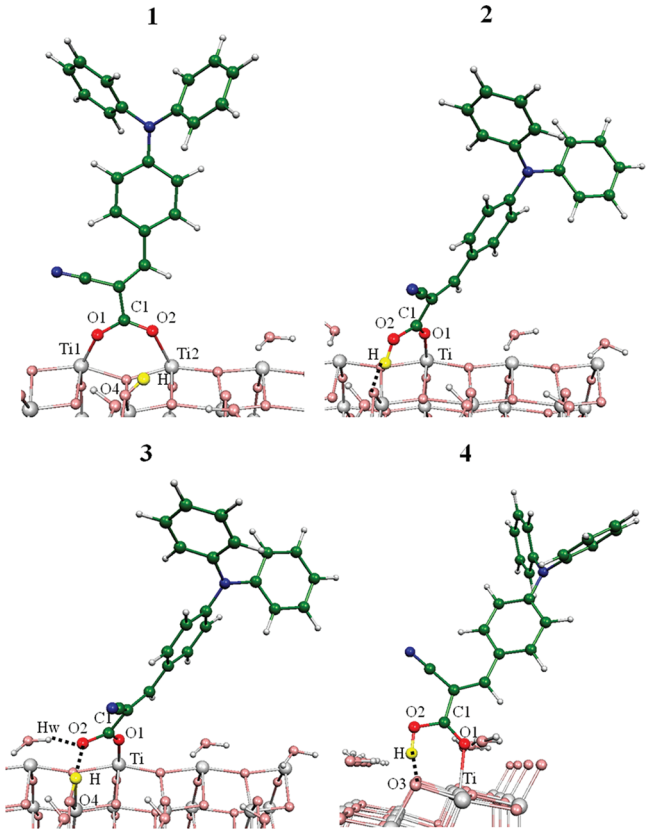

Figure 2. Optimized structured of [L0] coadsorbed with water: dissociative bidentate **1**, molecular monodentate **2**, dissociative monodentate **3**, and molecular monodentate **4**.

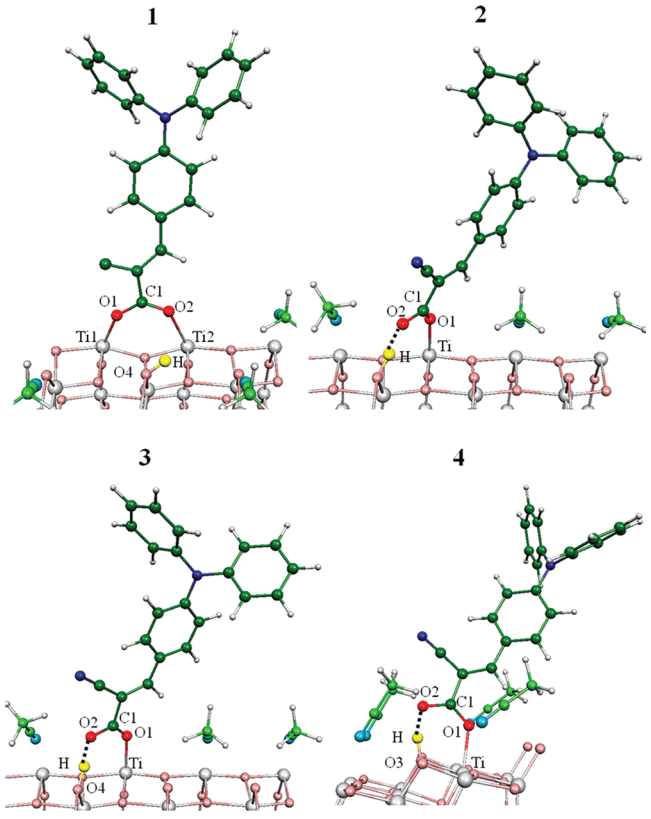

Figure 3. Optimized structures of [L0] coadsorbed with acetonitrile: dissociative bidentate **1**; dissociative monodentate structures **2**, **3**, and **4**.

geometry is similar to those of [BA] and isonicotinic acid in ref 34. Moreover, a binding energy difference of 7.4 kcal/mol between monodentate and bidentate isonicotinic acid was obtained in ref 34; this result is close to our computed energy difference of 6.9 kcal/mol in vacuo for the respective adsorption modes **1** and **4** of [BA].

Our calculations for [BA] adsorbed on the $(TiO_2)_{38}$ cluster are reported in the Supporting Information. It is worth noting that CP and ADF predict a slightly different relative stability for structures **1** and **4** of [BA] on the $(TiO_2)_{38}$ cluster, as they give an energy difference of 6.9 and 3.9 kcal/mol, respectively, in favor of **4**. The **2**−**4** energy difference is less sensitive to the employed method: 9.3 vs 10.7 kcal/mol. Interestingly, single-point CP calculations at the ADF-optimized geometry give almost the same **1**−**4** difference, 7.2 kcal/mol; see the Supporting Information. These data indicate that ADF and CP provide a somewhat different description of the acid−base energetics of the dye on the TiO_2 substrate.

In the presence of a water layer, the most stable geometry is the dissociated monodentate structure **3**, with adsorption energies of −16.8, −16.5, and −20.2 kcal/mol for [BA], [CA], and [L0], respectively. The adsorption energy and geometry that we obtain for [BA] with coadsorbed water are similar to those for adsorbed formic acid on hydrated TiO_2 reported in a recent theoretical work.[31] Also, in this case, the highest L0 binding energy within the series can be associated to the presence of the donor moiety, although the presence of water reduces the L0 binding energy by more than 3 kcal/mol.

In acetonitrile, the most stable configuration is the dissociated monodentate structure **4**, the computed adsorption energies being −13.5, −17.8, and −16.3 kcal/mol for [BA], [CA], and [L0], respectively. The adsorption energy for [L0] is thus further reduced by 4 kcal/mol compared with water. Moreover, for [L0], the adsorption energy of the bidentate structure **1** is very similar to that of the dissociative monodentate **4**. For this configuration, the highest adsorption energies are those of [CA] and [L0], which have the same cyanoacrylic anchoring group with the −CN moiety that is present also in acetonitrile. The similar adsorption energy can be associated with the interaction between the adsorbed CH_3CN on the TiO_2 surface and the −CN moiety of the dyes. This can induce a further stabilization during the adsorption leading to the same adsorption energy. [BA], which does not have the −CN group, shows a lower adsorption energy of about 3 to 4 kcal/mol in comparison with [CA] and [L0]. As shown in Table 2, for [L0], the adsorption energies of structures **1** and **4** in acetonitrile are similar (−15.7 and −16.3 kcal/mol, respectively), suggesting that the two adsorption modes have essentially the same probability of being present on the TiO_2 surface.

5. ADSORPTION OF A SOLVENT MONOLAYER

To gain insight into the effect of the solvent and the differences between water and acetonitrile, we also studied the TiO_2 surface fully covered with a monolayer of solvent molecules, saturating all of the five-coordinated Ti atoms of our (101) surface model. As we can see in Figure 4, water molecules are bound to Ti centers by their oxygen atoms, with average bond distances of 2.35 Å. The two water hydrogen atoms, H1 and H2, are involved in different hydrogen-bond interactions. Whereas H1 (Figure 4) points toward the oxygen belonging to

dx.doi.org/10.1021/jp209420h | J. Phys. Chem. C 2012, 116, 5932−5940

Table 2. Adsorption Energies for the Investigated Systems[a]

	ΔE_{ads} [kcal/mol]								
	[BA]			[CA]			[L0]		
	vac.	wat.	ac.	vac.	wat.	ac.	vac.	wat.	ac.
1	−14.2	−6.9	−9.0	−13.8	−8.7	−10.1	−17.6	−12.4	**-15.7**
2	−19.6	−11.5	−12.1	−18.6	−14.6	−11.9	−18.5	−11.1	−10.8
3	−19.3	**-16.8**	−10.6	−13.6	**-16.5**	−13.0	−11.1	**-20.2**	−8.5
4	**-21.1**	−13.1	**-13.5**	**-20.6**	−14.7	**-17.8**	**-23.4**	−16.3	**-16.3**

[a]Values in bold indicate the most stable structures.

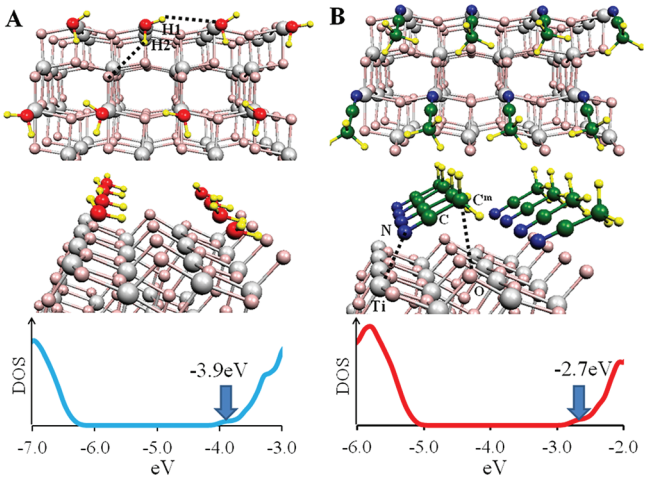

Figure 4. Optimized structures and DOS of the TiO_2 surface with an adsorbed monolayer of water (A) (blue line) and acetonitrile (B) (red line). A Gaussian broadening of 0.01 Ry is used.

a nearby water molecule with a distance comprised between 3.1 and 3.2 Å, the H2 atom (Figure 4) points toward the two-coordinated oxygen of the TiO_2 surface with a distance comprised between 2.50 and 3.0 Å. This structural result nicely agrees with previous theoretical work.[39]

Similarly, we studied the geometrical structure of TiO_2 covered by a monolayer of acetonitrile; see Figure 4. The acetonitrile molecules are bound to the five-coordinated Ti atoms through their nitrogen atoms. The average N−Ti and C^m-O_{2c} distances (Figure 4) are 2.44 and 3.42 Å, respectively, with a Ti−N−C angle of 144°. These results are in agreement with previous computational work.[42]

The results in Table 3 show that the adsorption energy of a single molecule of water is similar to that of a single molecule of acetonitrile (−17.4 vs −17.6 kcal/mol), whereas at full coverage the adsorption energy of water is higher than that of acetonitrile (−15.9 vs −9.0 kcal/mol per molecule). This can be attributed to the higher steric hindrance of acetonitrile compared with water. Moreover, the intermolecular hydrogen bond between adsorbed water molecules (see Figure 4A) further contributes to stabilizing the full-coverage monolayer formation.

Table 3. Adsorption Energy Per Molecule for a Single Solvent Molecule and a Full Monolayer of Solvent Molecules in Kilocalories Per Mole

coverage	H_2O	CH_3CN
single molecule	−17.4	−17.6
full coverage	−15.9	−9.0

By comparing the results in Table 3 to the dye adsorption energies in Table 2, we can approximately estimate the relative affinity of the dyes and the solvent molecules for anchoring on to the bare TiO_2 surface. Our results suggest that water can effectively compete with dye adsorption, whereas acetonitrile should be less effective in competing with the dye for the TiO_2 anchoring sites. This is in line with the impact of water contamination on the DSSC stability and supports the results of the Car−Parrinello molecular dynamics simulation in ref 22, where desorption of the dye was observed in the presence of bulk water solvation.

In Figure 4 we show the density of states (DOSs) for a slab covered by a full monolayer of water or acetonitrile. The absolute energy of the TiO_2 conduction band was determined by referring the Kohn−Sham eigenvalues to the value of the electrostatic potential in the vacuum region between consecutive slabs. (See the Supporting Information.) In the presence of water, we find an upward shift of the conduction band by 1.2 eV compared with that of the bare TiO_2 slab. This can be attributed to the donor character of the adsorbed water molecules, leading to an increase in the negative charge on the TiO_2 surface. A similar conduction band upshift (1.6 eV) upon hydration has also been obtained for rutile TiO_2 in the presence of a water monolayer,[46] and a further (0.5 to 0.6 eV) upshift of the conduction band was found with increasing water coverage.[46] The energy level of the conduction band with up to a monolayer of water reported in ref 46 (−4.3 eV) and calculated by us (−3.9 eV) is in good agreement with the experimental measurement of −4.1 eV.[1d]

In the presence of an acetonitrile monolayer, our calculations show an additional upshift of the TiO_2 CB of 1.2 eV relative to the water case. By comparing the calculated band gap of the bare and the solvated TiO_2 with a monolayer of acetonitrile, we find a very slight variation (<0.1 eV), in agreement with a previous computational study.[50] The computed CB upshift in acetonitrile relative to water compares favorably with the values of Fitzmaurice and coworkers,[24−27] even though our calculations do not include the effects of surface protonation and bulk solvation, which could also affect the position of the TiO_2 CB.

6. ELECTRONIC STRUCTURE OF DYE-SENSITIZED TiO_2 IN THE PRESENCE OF THE SOLVENT

Although the employed computational setup, in particular, the use of a GGA exchange-correlation functional, is known to be problematic in describing the alignment of energy levels at dye−semiconductor interfaces,[60] the relative level shifts observed in the TiO_2 conduction band states from vacuo to solvent are expected to be significant. For comparative purposes, in Figure 5, we report the computed DOS for the most stable optimized structures of [BA], [CA], and [L0]

dx.doi.org/10.1021/jp209420h | J. Phys. Chem. C 2012, 116, 5932−5940

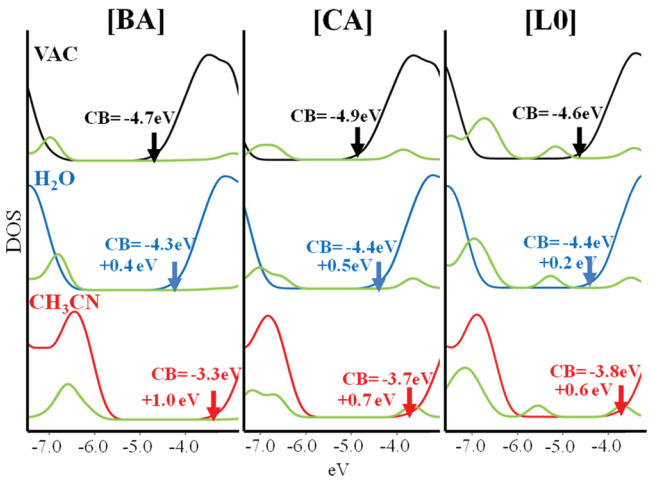

Figure 5. Density of states (DOS) for the three investigated TiO_2/dye systems in vacuo (black line), in water (blue line), and in acetonitrile (red line). Green lines represent the contribution of the adsorbed molecules to the density of states (PDOS). The energies are referred to the vacuum level.

adsorbed on TiO_2 in vacuo, water, and acetonitrile. The absolute energy of the TiO_2 conduction band was determined by referring the Kohn−Sham eigenvalues to the vacuum level, as determined from the value of the electrostatic potential in the vacuum region of the supercell. In the Supporting Information, we report the electrostatic potentials along the direction normal to the surface for the dye-sensitized TiO_2 slab in vacuo and in the presence of the solvent (water and acetonitrile, alternatively). By comparing the CB level of the bare and the dye-sensitized TiO_2 in vacuo, we find differences in the behavior of the three investigated molecules. As previously described, it is the sensitizer's dipole component normal to the surface that induces a shift in the TiO_2 CB energy.[11,61] To gain insight into the effect of the dipole moment of the adsorbed molecules on the TiO_2 conduction band energy, we performed single-point calculations on the isolated [BA], [CA], and [L0] in their adsorption geometry using the Gaussian03 package[62] (B3LYP/6-31G*). The resulting values of the dipole moment for [BA], [CA], and [L0] are +1.9, 0.0, and +2.7 D, whereas the CB shifts with respect to the bare TiO_2 are +0.3, +0.1, and +0.4 eV, respectively.

Concerning the effect of the coadsorbed solvent, the TiO_2 conduction band in the presence of water is upshifted by 0.2 to 0.5 eV compared with the value in vacuo. In the presence of acetonitrile, the upshift is 0.6 to 1.0 eV relative to that in water. Therefore, the presence of the dyes modulates the TiO_2 conduction band upshift, decreasing the shifts found without dyes. Moreover, specific dye/acetonitrile interactions may give rise to the differences in the shifts found for the three dyes in this solvent, with L0 showing the lowest shift. In any case, also for the dye-sensitized interfaces, the presence of acetonitrile contributes to raise the TiO_2 CB, which should be beneficial for the DSSCs performance in terms of open circuit voltage.

7. CONCLUSIONS

A first-principles investigation has been carried out to gain insight into the effects of explicit solvent (water and acetonitrile) molecules on the adsorption energy and electronic structure of organic dye molecules adsorbed on the TiO_2 anatase (101) surface. The selected systems are prototype examples of dyes anchoring with a carboxylic ([BA]) or cyanoacrylic ([CA] and [L0]) moieties. We investigated altogether one bidentate and three monodentate (both molecular and dissociative) structures, in vacuo and in the presence of one layer of coadsorbed solvent molecules. From the calculated energies, the most stable structure in vacuo is a molecular monodentate structure, whereas in the presence of coadsorbed water the most stable structure is a dissociated monodentate configuration. In acetonitrile, a different dissociated monodentate structure is found, with essentially the same binding energy of the bidentate structure. (Actually, the relative stabilities of these two adsorption modes are sensitive to the level of calculation.) Our systematic study shows important effects of the solvent on the dye adsorption geometry: (i) the adsorbed solvent induces the deprotonation of the dye due to the changing the acid/base properties of the system; (ii) the solvent increases the bonding distance of the dye from the Ti anchoring atoms, reducing the dye adsorption energy; and (iii) the O−C−O bonds in the carboxylic moieties become more symmetric than in vacuo.

Analysis of the electronic structure for the most stable configurations shows the crucial effect of explicit solvation on the position of the TiO_2 conduction band. The TiO_2 conduction band in the presence of water is upshifted by 0.2 to 0.5 eV compared with the vacuo and downshifted by 0.6 to 1.0 eV compared with acetonitrile. The differences between water and acetonitrile can be related to two aspects: (i) the dipole of the acetonitrile molecules pointing with the negative charge toward the TiO_2 surface and (ii) the donor role of the acetonitrile −CN group with respect to the reactive Ti atoms. Even with the limitations of the model and the approximation employed in our simulations, the overall picture extracted from our calculations is consistent with conduction band upshift measured in acetonitrile compared with water, as from the classical papers by Fitzmaurice and coworkers[24−27] and suggests a relevant role of solvation in determining the dye−semiconductor electronic coupling. Further studies are in progress to include the effect of surface protonation and of bulk solvation on the position of the TiO_2 conduction band.

■ ASSOCIATED CONTENT

Supporting Information

Optimized geometrical structures of the [BA] and [CA] systems. Comparative results using a cluster approach. Electrostatic potential plots. This material is available free of charge via the Internet at http://pubs.acs.org.

■ AUTHOR INFORMATION

Corresponding Author

*E-mail: aselloni@princeton.edu, filippo@thch.unipg.it.

Notes

The authors declare no competing financial interest.

■ ACKNOWLEDGMENTS

E.M. and F.D.A. thank FP7-ENERGY-2010 project 261920 "ESCORT" and Istituto Italiano di Tecnologia, Project Seed 2009 "HELYOS" for financial support. A.S. acknowledges support by DoE-BES, Chemical Sciences Geosciences and Biosciences Division (DE-FG02-05ER15702). Princeton Tigress facilities are acknowledged for CPU time.

REFERENCES

(1) (a) O'Regan, B.; Grätzel, M. *Nature* **1991**, *353*, 737−740. (b) Hagfeldt, A.; Boschloo, G.; Sun, L.; Kloo, L.; Pettersson, H. *Chem. Rev.* **2010**, *110*, 6595−6663. (c) Grätzel, M. *Acc. Chem. Res.* **2009**, *42*, 1788−1798. (d) Grätzel, M. *Nature* **2001**, *414*, 338−344.

(2) Murakoshi, K.; Kano, G.; Wada, Y.; Yanagida, S.; Miyazaky, H.; Matsumoto, M.; Murasawa, S. *J. Electronal. Chem.* **1995**, *396*, 27−34.

(3) Bach, U.; Lupo, D.; Comte, P.; Moser, J. E.; Weissortel, F.; Salbeck, J.; Spreitzer, H.; Grätzel, M. *Nature* **1998**, *395*, 583−585.

(4) Hagfeldt, A.; Didriksson, B.; Palmquist, T.; Lindström, H.; Södergren, S.; Rensmo, H.; Lindsquist, S. *Sol. Energy Mater. Sol. Cells* **1994**, *31*, 481−488.

(5) Boschloo, G.; Lindström, J; Magnussom, E.; Holmberg, A.; Hagfeldt, A. *J. Photochem. Photobiol., A* **2002**, *148*, 11−15.

(6) Nazeeruddin, M.; Kay, A.; Rodicio, I.; Humphry-Baker, R.; Muller, E.; Liska, P.; Vlachopoulos, N.; Grätzel, M. *J. Am. Chem. Soc.* **1993**, *115*, 6382−6390.

(7) Nazeeruddin, M.; Pechy, P.; Renouard, T.; Zakeeruddin, S.; Humphry-Baker, R.; Comte, P.; Liska, P.; Cevey, L.; Costa, E.; Shklover, V.; et al. *J. Am. Chem. Soc.* **2001**, *123*, 1613−1624.

(8) Nazeeruddin, M.; De Angelis, F.; Fantacci, S.; Selloni, A.; Viscardi, G.; Liska, P.; Ito, S.; Takeru, B.; Grätzel, M. *J. Am. Chem. Soc.* **2005**, *127*, 16835−16847.

(9) Fukui, A.; Ryoichi, K.; Yamanaka, R.; Islam, A.; Han, L. *Sol. Energy Mater. Sol. Cells* **2006**, *90*, 649−658.

(10) Lee, K. M.; Suryanarayanan, V.; Ho, K. C. *J. Power Sources* **2009**, *188*, 635−641.

(11) Chen, P.; Yum, J. H.; De Angelis, F.; Mosconi, E.; Fantacci, S.; Moon, S.-J.; Baker, R. H.; Ko, J.; Nazeeruddin, M. K.; Grätzel, M. *Nano Lett.* **2009**, *9*, 2487−2492.

(12) De Angelis, F.; Fantacci, S.; Selloni, A.; Grätzel, M.; Nazeeruddin, M. K. *Nano Lett.* **2007**, *7*, 3189−3895.

(13) Tropsha, T. G.; Harvey, N. G. *J. Phys. Chem. B* **1997**, *101*, 2259−2266.

(14) Liu, Y.; Hagfeldt, A.; Xiao, X.-R.; Lindquist, S.-E. *Sol. Energy Mater. Sol. Cells* **1998**, *55*, 267−281.

(15) Hui, Z.; Xiong, Y.; Heng, L.; Yuan, L.; Yu-Xiang, W. *Chin. Phys. Lett.* **2007**, *24*, 3272−3275.

(16) Lu, H.-L.; Lee, Y.-H.; Huang, S.-T.; Su, C.; Yang, T. C.-K. *Sol. Energy Mater. Sol. Cells* **2011**, *95*, 158−162.

(17) Jung, Y.-S.; Yoo, B.; Lim, M. K.; Lee, S. Y.; Kim, K.-J. *Electrochem. Acta* **2009**, *54*, 6286−6291.

(18) Hahlin, M.; Johansson, E. M. J.; Schölin, R.; Siegbahn, H.; Rensmo, H. *J. Phys. Chem. C* **2011**, *115*, 11996−12004.

(19) Mikoshiba, S.; Murai, S.; Sumino, H.; Kado, T.; Kosugi, D.; Hayase, S. *Curr. Appl. Phys.* **2005**, *5*, 152−158.

(20) Weidmann, J.; Dittrich, T.; Konstantinova, E.; Lauermann, I.; Uhlendorf, I.; Koch, F. *Sol. Energy Mater. Sol. Cells* **1998**, *56*, 153−165.

(21) Mikoshiba, S.; Murai, S.; Sumino, H.; Hayase, S. *Chem. Lett.* **2002**, *12*, 1156−1157.

(22) De Angelis, F.; Fantacci, S.; Gebauer, R. *J. Phys. Chem. Lett.* **2011**, *2*, 813−817.

(23) Lee, K.-M.; Suryanarayanan, V.; Ho, K.-C. *J. Power Sources* **2009**, *188*, 635−641.

(24) Redmond, G.; Fitzmaurice, D. *J. Phys. Chem.* **1993**, *97*, 1426−1430.

(25) Rothenberger, G.; Fitzmaurice, D.; Grätzel, M. *J. Phys. Chem.* **1992**, *96*, 5983−5986.

(26) O'Regan, B.; Grätzel, M.; Fitzmaurice, D. *J. Phys. Chem.* **1991**, *95*, 10525−10528.

(27) Boschloo, G.; Fitzmaurice, D. *J. Phys. Chem. B* **1999**, *103*, 7860−7868.

(28) Li, W.-K.; Gong, X.-Q.; Lu, G.; Selloni, A. *J. Phys. Chem. C* **2008**, *112*, 6594−6596.

(29) Gong, X.-Q.; Selloni, A.; Vittadini, A. *J. Phys. Chem. B* **2006**, *110*, 2804−2811.

(30) Vittadini, A.; Selloni, A.; Rotzinger, F. P.; Grätzel, M. *J. Phys. Chem. B* **2000**, *104*, 1300−1306.

(31) Miller, K. L.; Musgrave, C. B.; Falconer, J. L.; Medlin, J. W. *J. Phys. Chem. C* **2011**, *115*, 2738−2749.

(32) Miller, K. L.; Falconer, J. L.; Medlin, J. W. *J. Catal.* **2011**, *278*, 321−328.

(33) (a) Martsinovich, N.; Jones, D. R.; Troisi, A. *J. Phys. Chem. C* **2010**, *114*, 22659−22670. (b) Martsinovich, N.; Troisi, A. *Energy Environ. Sci.* **2011**, *4*, 4473−4495.

(34) Nilsing, M.; Persson, P.; Ojamäe, L. *Chem. Phys. Lett.* **2005**, *415*, 375−380.

(35) Hirva, P.; Haukka, M. *Langmuir* **2010**, *26*, 17075−17081.

(36) Bermudez, M. *Surf. Sci.* **2010**, *604*, 706−712.

(37) Rocca, D.; Gebauer, R.; De Angelis, F.; Nazeeruddin, M. K.; Baroni, S. *Chem. Phys. Lett.* **2009**, *475*, 49−53.

(38) Pastore, M.; De Angelis, F. *ACS Nano* **2010**, *4*, 556−562.

(39) (a) Srinivas, K.; Sivakumar, G.; Kumara, Ch. R.; Reddy, M. A.; Bhanuprakash, K.; Rao, V. J.; Chen, C.-W.; Hsu, Y.-C.; Lin, J. T. *Synth. Met.* **2011**, *161*, 1671−1681. (b) Martsinovich, N.; Troisi, A. *J. Phys. Chem. C* **2011**, *115*, 11781−11792.

(40) De Angelis, F.; Fantacci, S.; Selloni, A.; Nazeeruddin, M. K.; Grätzel, M. *J. Phys. Chem. C* **2010**, *114*, 6054−6061.

(41) De Angelis, F.; Fantacci, S.; Selloni, A.; Nazeeruddin, M. K.; Grätzel, M. *J. Am. Chem. Soc.* **2007**, *129*, 14156−14157.

(42) (a) De Angelis, F.; Fantacci, S.; Mosconi, E.; Nazeeruddin, M. K.; Grätzel, M. *J. Phys. Chem. C* **2011**, *115*, 8825−8831. (b) Labat, F.; Ciofini, I.; Hratchian, H. P.; Frisch, M. J.; Raghavachari, K.; Adamo, C. *J. Phys. Chem. C* **2011**, *115*, 4297−4306.

(43) Tilocca, A.; Selloni, A. *Langmuir* **2004**, *20*, 8379−8384.

(44) Li, W.-K.; Gong, X.-Q.; Lu, G.; Selloni, A. *J. Phys. Chem. C* **2008**, *112*, 6594−6595.

(45) Cheng, H.; Selloni, A. *Langmuir* **2010**, *26*, 11518−11525.

(46) Cheng, J.; Sprik, M. *Phys. Rev. B* **2010**, *82*, 081406.

(47) Schiffmann, F.; Hutter, J.; Vondele, J. V. *J. Phys.: Condens. Matter* **2008**, *20*, 064206.

(48) Schiffmann, F.; Vondele, J. V.; Hutter, J.; Urakawa, A.; Wirz, R.; Baiker, A. *Proc. Natl. Acad. Sci. U.S.A.* **2010**, *107*, 4830−4833.

(49) Schiffmann, F.; Vondele, J. V.; Hutter, H. J.; Wirz, R.; Urakawa, A.; Baiker, A. *J. Phys. Chem. C* **2010**, *114*, 8398−8404.

(50) Sumita, M.; Sodeyama, K.; Han, L.; Tateyama, Y. *J. Phys. Chem. C* **2011**, *115*, 19849−19855.

(51) Pastore, M.; Mosconi, E.; De Angelis, F.; Grätzel, M. *J. Phys. Chem. C* **2010**, *114*, 7205−7212.

(52) Hagberg, D. P.; Marinado, T.; Karlsson, K. M.; Nonomura, K.; Qin, P.; Boschloo, G.; Brinck, T.; Hagfeldt, A.; Sun, L. *J. Org. Chem.* **2007**, *72*, 9550−9556.

(53) Perdew, J.; P.; Burke, K.; Ernzerhof, M. *Phys. Rev. Lett.* **1996**, *77*, 3865−3868.

(54) Giannozzi, P.; Baroni S.; Bonini, N.; Calandra, M.; Car, R.; Cavazzoni, C.; Ceresoli, D.; Chiarotti, G. L.; Cococcioni, M.; Dabo, I.; et al. *J. Phys.: Condens. Matter*, **2009**, *21*, 395502.

(55) te Velde, G.; Bickelhaupt, F. M.; Baerends, E. J.; Fonseca Guerra, C.; van Gisbergen, S. J. A.; Snijders, J. G.; Ziegler, T. *J. Comput. Chem.* **2001**, *22*, 931−967.

(56) Persson, P.; Bergstrom, R.; Lunell, S. *J. Phys. Chem. B* **2000**, *104*, 10348−10351.

(57) De Angelis, F.; Tilocca, A.; Selloni, A. *J. Am. Chem. Soc.* **2004**, *126*, 15024−15025.

(58) (a) Lundqvist, M. J.; Nilsing, M.; Lunell, S.; Akemark, B.; Persson, P. *J. Phys. Chem. B* **2006**, *110*, 20513−20525. (b) Lundqvist, M. J.; Nilsing, M.; Persson, P.; Lunell, S. *Int. J. Quantum Chem.* **2006**, *106*, 3214−3234.

(59) Vittadini, A.; Selloni, A.; Rotzinger, F. P.; Gräztel, M. *Phys. Rev. Lett.* **1998**, *81*, 2954−2957.

(60) (a) Montanari, B.; Harrison, N. M. *Chem. Phys. Lett.* **2002**, *364*, 529−534. (b) Muscat, J.; Wander, A.; Harrison, N. M. *Chem. Phys. Lett.* **2001**, *342*, 397−401.

(61) Rühle, S.; Greenshtein, M.; Chen, S. G.; Merson, A.; Pizem, H.; Sukenik, C. S.; Cahen, D.; Zaban, A. *J. Phys. Chem. B* **2005**, *109*, 18907−18913.

(62) Frisch, M. J.; Trucks, G. W.; Schlegel, H. B.; Scuseria, G. E.; Robb, M. A.; Cheeseman, J. R.; Montgomery, Jr., J. A.; Vreven, T.; Kudin, K. N.; Burant, J. C.; et al. *Gaussian 03*; Gaussian, Inc.: Pittsburgh, PA, 2003.